COMPDYN 2011
III ECCOMAS Thematic Conference on
Computational Methods in Structural Dynamics and Earthquake Engineering
M. Papadrakakis, M. Fragiadakis, V. Plevris (eds.)
Corfu, Greece, 25–28 May 2011

DAMAGE IDENTIFICATION FOR A REDUCED SCALE SPATIAL STEEL FRAME

Michele Betti[1], **Paolo Biagini**[1], **and Luca Facchini**[1]

[1] University of Florence, Department of Civil and Environmental Engineering
Via S. Marta 3 – 50139 Florence – Italy
e-mail: mbetti@dicea.unifi.it, paolo.biagini@dicea.unifi.it, luca.facchini@unifi.it

Keywords: Steel-Frame Structures, Damage Identification, Health Monitoring, Stochastic Subspace Identification.

Abstract. *This paper reports on an experiment carried out in the laboratory of Civil and Environmental Engineering of the University of Florence, where a reduced scale (approximately 2.5 m width × 2.5 m depth × 4.8 m height), three storey steel spatial frame was instrumented and progressively damaged by cutting one of its pillars just above the foundation; the deepness of the cut could be measured and was taken as the entity of the damage. A series of 12 accelerometers was installed on the frame and 3 more accelerometers were installed on the ground; acceleration measurements induced by ambient vibrations were recorded as the frame was progressively damaged. Acceleration signals were subsequently analyzed in both time and frequency domain (SSI, EFDD, neural networks): a frequency shift and a change in the corresponding modal shapes were observed as the damage increased. The damaged truss was also modelled by means of a FEM code and the frequency shift and the change in the modal shapes were reproduced. A genetic algorithm approach is currently being tested to try and indentify the location and entity of the damage, and is reported on.*

1 INTRODUCTION

Safety evaluation and damage assessment of existing engineering structures asks for a deeper structural analysis; usually this investigation is carried out through the finite element method techniques: a numerical model of the structure simulates the behavior of the structure (both in static and dynamic field) and it is used to predict the building response to service and exceptional loads (such as earthquakes). The correct identification of the numerical model is then a fundamental task as the modeling, even if refined from a geometrical point of view, could differ from the real structural behavior if assumptions on material, constraints, masses and stiffness are not properly evaluated. Variability of these elements can produce results that could be substantially different from the actual behavior of the structure.

To properly identify the numerical model several strategies, or methodologies, are available in the inherent literature. An effective approach to assess the structural behavior is to evaluate, by performing dynamic experimental tests, actual modal frequencies and corresponding mode shapes. Dynamic tests could be made assuming both forced (vibrodine) and/or environmental (wind or traffic) loads. This step is interesting also with respect to the so-called Structural Health Monitoring (SHM) [1] [2]. The evaluation of these quantities becomes a classical "output-only identification" problem. The identification of the FE model can thus be seen as an optimization strategy where the cost function could be assumed, f.i., the distance between the modal frequencies and mode shape obtained by experimental dynamic tests and those obtained by the numerical model. To address this optimization several approaches have been proposed in literature; among the others quite recently Facchini *et al.* [3] [4] propose a neural network approach. The "output-only" procedure could be framed as an emerging topic of both the scientific and technical community as it covers a wide range of practical problems. Effective examples can be considered, for instance, any situation where the need is felt to maintain the structure at hand operative during structural health monitoring investigation: this is the case of bridges which have to remain open to traffic during the test, as well as offshore structures (both small and medium size) ([4]) where the transport of the equipment needed for the monitoring can be extremely difficult.

In structural engineering field the most expeditive (but also, in some respects, the most "brutal") method to approach the identification problems in case of "output only" systems is the Peak – Picking method (see e.g. Bendat & Piersol 1993 [5]). After the evaluation of the Fourier transform of the recorded signals, the eigen-frequencies of the investigated structure are assessed searching the peaks in the spectrum plot. The eigen-modes can then be determined by comparing the transfer functions of the various recordings with a reference one. The method has the advantage of being relatively simple, however in the case of complex structures it might not be able to provide significant results due to the fact that, of course, it depends on the sensitivity of the operator who has to recognize the peak of auto-spectral density. Despite its disadvantages the popularity of the method is mainly due to its simplicity as the only algorithm that is needed to convert time data to spectra is the Fast Fourier Transform (FFT).

In the last decade more advanced methods, even if more computational demanding, have been proposed. Among them it is noteworthy to remember the so-called SSI (Stochastic Subspace Identification) (see e.g. Peeters & De Roeck 1996 [6]). Starting from the consideration that in many cases of engineering interest is extremely difficult, if not impossible, to have a deterministic knowledge of the forcing process (environmental loads) the method assume a stochastic loading (often a white noise). Many applications of SSI were presented in the scientific literature showing the attractiveness of the method.

Figure 1: Three-storey investigated steel building.

The paper, discussing these problems, presents a technique for the identification of "output only" systems by means of neural networks. In a first part of the paper the experimental campaign conducted in a benchmark three-storey steel structure built at the Civil Engineering Laboratory of the University of Florence (Italy). The structure has been tested under ambient loading starting from the undamaged configuration and imposing steps of increasing damage level by incremental cuts on a steel column: the tests have been performed assuming the building being initially undamaged; successively, incremental damage states have been imposed by partially cutting one of the columns and test have been repeated. Then, a neural network based procedure has been developed to analyze accelerometer signals recorded during the experimental campaign. Results are discussed and the dynamic properties of the building are evaluated at each damage level. At the end, the ongoing research aimed to employ genetic algorithms to the structural system identification is discussed.

2 EXPERIMENTAL LAYOUT

2.1 The specimen

The case study is a three-storey steel structure (Figure 1) with profiled steel elements; this specimen has been analysed starting from an undamaged configuration and imposing increasing damage level (by progressive cutting of a column flanges).

The plane dimension of the steel frame is 2.5 m × 2.5 m. The height of the first storey is 1.64 m, while is 1.6 m for 2nd story and 1.54 for 3rd storey. The total height of the structure is 4.87 m. The layout of the specimen is shown in Figure 7. The material of steel elements was grade S235 steel with a nominal yield stress of 235 MPa. At each level a mass of about 22 kN was applied by means of concrete slabs (Figure 1) which have no structural function. The beam-to-column connections were fully welded to ensure rigidity. Column base connec-

tions were made as rigid as possible. The cross section of steel members is as follows: a) column HEB140; b) beam IPE 140; geometrical properties of member are reported in Table 1.

Properties	Columns	Beam
Section type	HEB140	IPE 140
Cross sectional area (cm^2)	42.96	16.43
	Moments of inertia (cm^4)	
Strong direction	1509	541.2
Weak direction	549.7	44.92

Table 1: Sectional properties of the structural members.

2.2 Ambient vibration test

To determine the vibration characteristics (natural frequencies and mode shapes) of the steel building model a series of ambient vibration tests were conducted.

A total of 12 uniaxial seismic accelerometers were installed on the frame (Figure 2); in particular at each level of the specimen 4 sensors have been placed to collect acceleration along the two main horizontal dimensions). The accelerometers are characterized by a 10 V/g sensitivity and a 0.1–1500 Hz frequency range.

Figure 2: Accelerometers disposition (level #1).

Test	Type of test	Load
Test # 1÷ 5	Without damage	Environmental
Test # 11÷13	Damage Level #1	Environmental
Test # 21÷23	Damage Level #2	Environmental
Test # 31÷33	Damage Level #3	Environmental
Test # 41÷43	Damage Level #4	Environmental

Table 2: Experimental campaign.

The sampling frequency during the experiment was 400 Hz and the measurement duration was selected as about 4 min for each test considering the vibration source. Table 2 reports a summary of the tests executed during the experimental campaign. The tests were performed starting from the specimen in its undamaged configuration and were repeated at four different levels of increasing damage (Figure 3÷Figure 4). The damage consisted in a progressive cut of the column flanges, as shown in Figure 3 to Figure 6.

Figure 3: Damage Level #1 (left) and Damage Level #3 (right).

Figure 4: Damage Level #4.

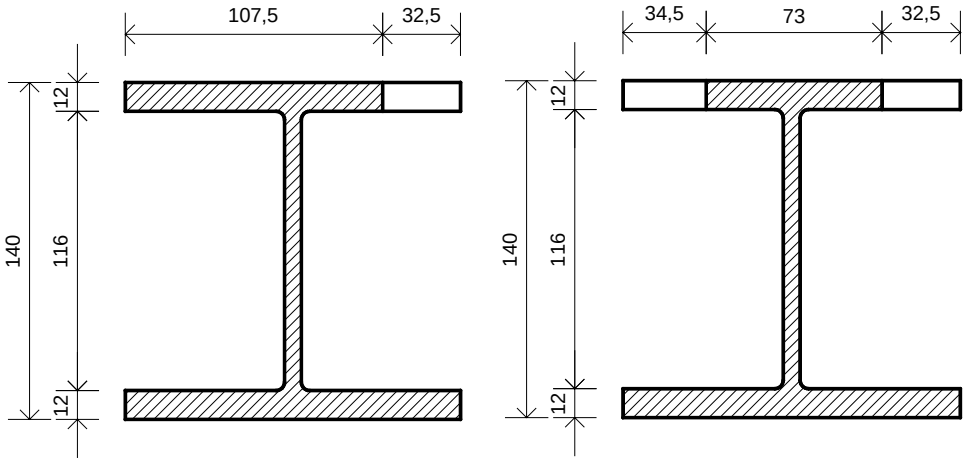

Figure 5: Damage Level # 1 and 2.

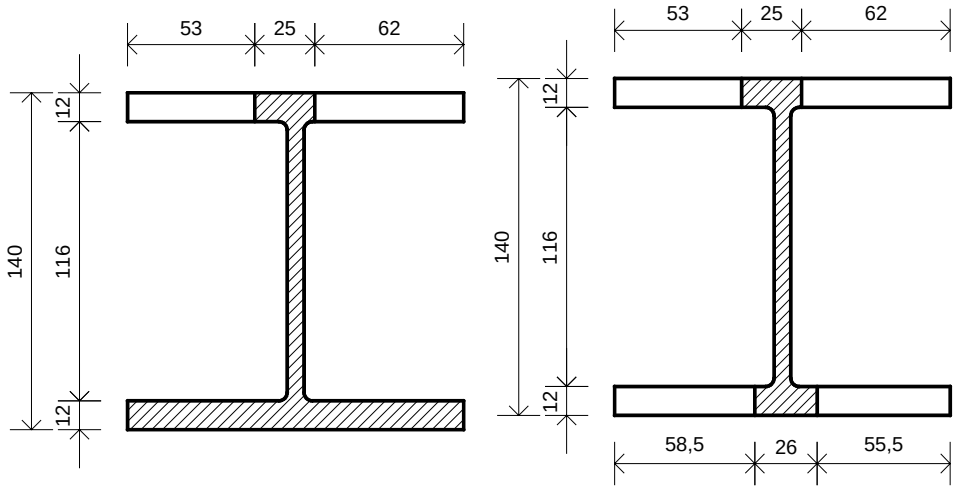

Figure 6: Damage Level # 3 and 4.

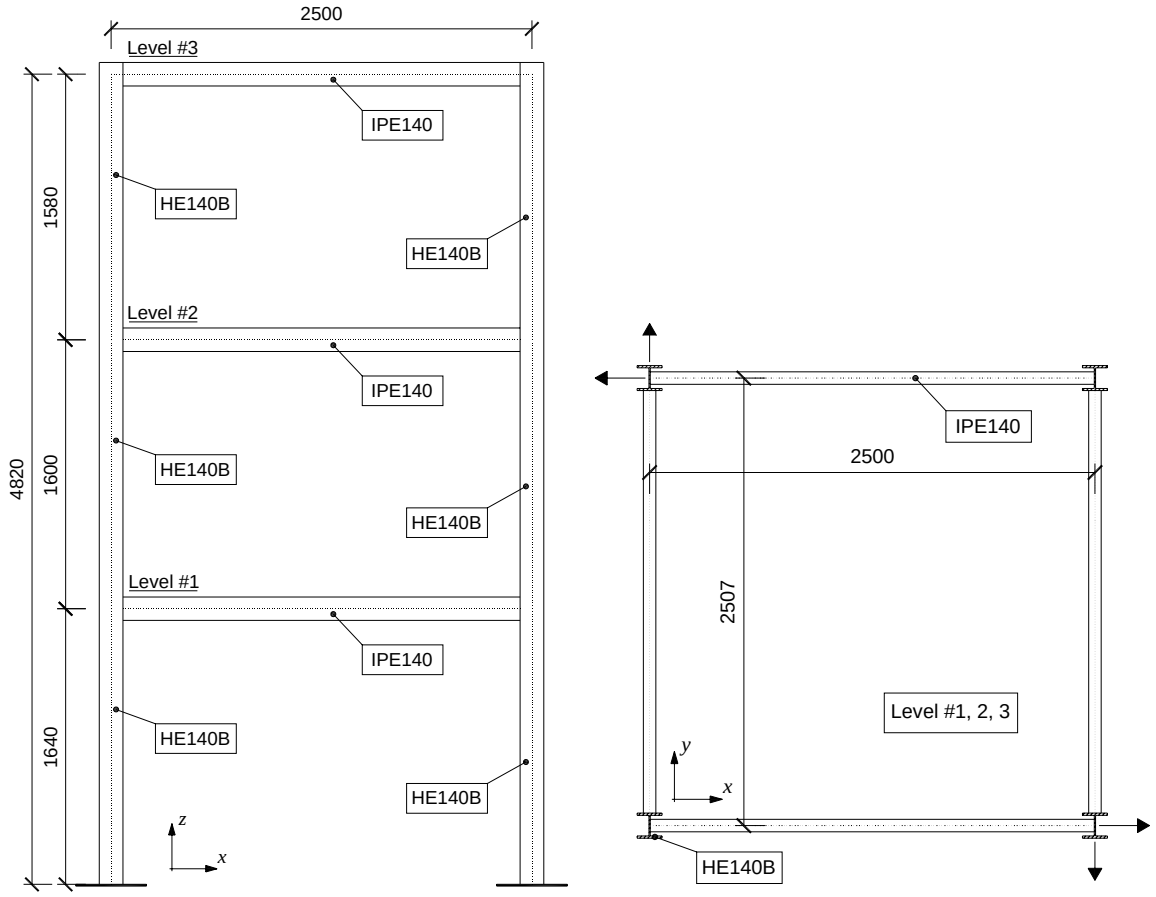

Figure 7. Specimen layout (mm).

3 NETWORK TRAINING AND SIGNAL ANALYSIS

The recognition of the structural eigenfrequencies was assisted by a neural network (described later) fed with four frequency-dependent indexes which summarize the behavior of the spectral tensor at each frequency of interest.

As a matter of fact, the response of structures with well separated eigenfrequencies and relatively low damping, when excited by random forcing processes, exhibit a spectral tensor characterized, in correspondence with the structural eigenfrequencies, by:

- the possibility to be decomposed in the tensor product of the corresponding modal shape by itself;
- a high coherence between any couple of degrees of freedom;
- a phase close to zero or to a multiple of π between any couple of degrees of freedom;
- the presence of peaks in the auto-spectral densities.

These four conditions enable to define four indexes which describe a kind of "degree of fulfillment" for each condition; the indexes were defined as follows.

The possibility to decompose the spectral tensor in the tensor product of a vector by itself can be readily checked by means of a singular value decomposition; the spectral theorem ensures that, at each frequency f of interest, the spectral tensor of the degrees of freedom can be decomposed as:

$$S(f) = \sum_{h=1}^{N} \lambda_h(f) \boldsymbol{\varphi}^{(h)}(f) \otimes \boldsymbol{\varphi}^{(h)}(f) \tag{1}$$

where $\lambda_h(f)$ are the eigenvalues and $\boldsymbol{\varphi}^{(h)}(f)$ the corresponding eigenvectors. When an eigenvalue is much greater than the others the spectral tensor reduces to:

$$S(f) \approx \lambda_1(f) \boldsymbol{\varphi}^{(1)}(f) \otimes \boldsymbol{\varphi}^{(1)}(f) \tag{2}$$

where, without loss in generality, the eigenvalues are considered to be sorted in descending order. The first index can therefore be defined as:

$$i_1(f) = \max\left\{0 \quad 1 - \frac{\left\| S(f) - \lambda_1(f) \boldsymbol{\varphi}^{(1)}(f) \otimes \boldsymbol{\varphi}^{(1)}(f) \right\|}{\left\| S(f) \right\|}\right\} \tag{3}$$

The degree of coherence between the various couples of signals can be checked by computing the norm of the coherence tensor; therefore the second index is defined as

$$i_2(f) = \frac{\left\| \mathbf{C}(f) \right\|}{N_{dof}} \tag{4}$$

where $\mathbf{C}(f)$ is the coherence tensor at each frequency of interest and N_{dof} the number of degrees of freedom of the structure.

The third index is a measure of the norm of the phase angle tensor, modulus π:

$$i_3(f) = \max\left\{0 \quad 1 - \frac{\left\|\Phi(f) \bmod \pi\right\|}{N_{dof}}\right\} \tag{5}$$

The fourth index is derived from an index reported in Deraemaeker *et al.* (2008) [1], and is the peak index. Denoting with $S_i(f)$ the auto-spectral density to be analyzed to evaluate the peaks it is possible to define the following quantities:

$$K(f_c) = \left[\int_{f_c-\Delta f}^{f_c+\Delta f} S_i(f)\, df\right]^{-1} \; ; \; \widetilde{S}_i(f_c, f) = K(f_c) S_i(f)$$

$$\mu(f_c) = \int_{f_c-\Delta f}^{f_c+\Delta f} f\, \widetilde{S}_i(f_c, f) df \; ; \; \sigma^2(f_c) = \int_{f_c-\Delta f}^{f_c+\Delta f} [f - \mu(f_c)]^2\, \widetilde{S}_i(f_c, f) df$$

The peak index is eventually defined by:

$$\lambda_4(f) = 1 - \frac{f_c\sqrt{3}}{\Delta f}\frac{\sigma(f)}{\mu(f)} \tag{6}$$

Since as many peak indexes can be evaluated as the number of degrees of freedom, the maximum of the various indexes is taken at each frequency.

3.1 Network definition and training

The utilized network was a feed-forward back-propagation network characterized by two-hidden layers with variable number of neurons: in particular, the behavior of networks with 5, 10 or 15 neurons in both hidden layers was inspected. Hidden neurons were characterised by sigmoid activation functions.

The input layer was always composed by 4 neurons, each accepting one of the indexes i_1 to i_4. The output layer computed a linear combination of the outputs of the second layer of neurons and gave the network output, i.e. an estimate $L(f)$ of the likelihood of finding a structural resonance at frequency f.

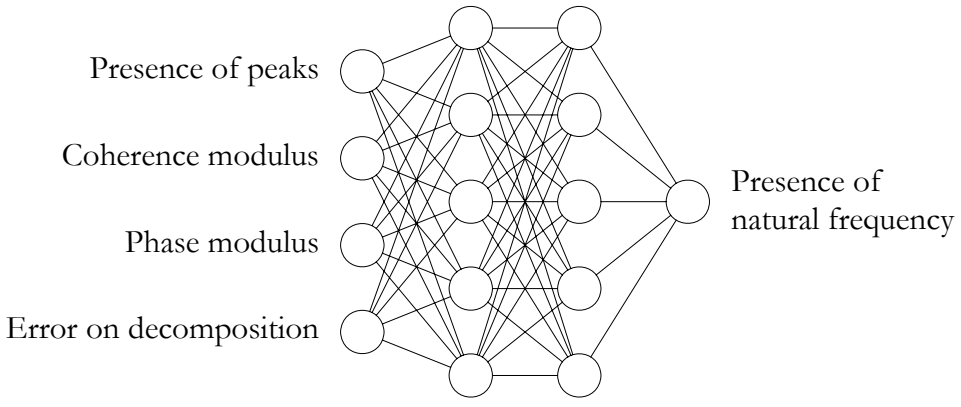

Figure 8: Example of neural architecture; here a 4-5-5-1 network is shown.

One of the major advantages of feeding the network with the four above-mentioned indexes is that training of neural network can be performed on a completely different structure,

as the indexes characteristics are widely general. The possibility of training the network on a generic structure overcomes the problem that the examined structure is still widely unknown, and moreover the training structure can be built numerically, thus perfectly knowing its dynamical characteristics.

Nevertheless, the network was trained on the results obtained for the FEM model of the investigated frame *prior* to identification. In other words, a FEM model was first built on the basis of the available information for the geometry and material. Once defined the stiffness and mass matrices of the model, the frequency response functions could be evaluated, together with the first eigenfrequencies and associated modal shapes (see Figure 9).

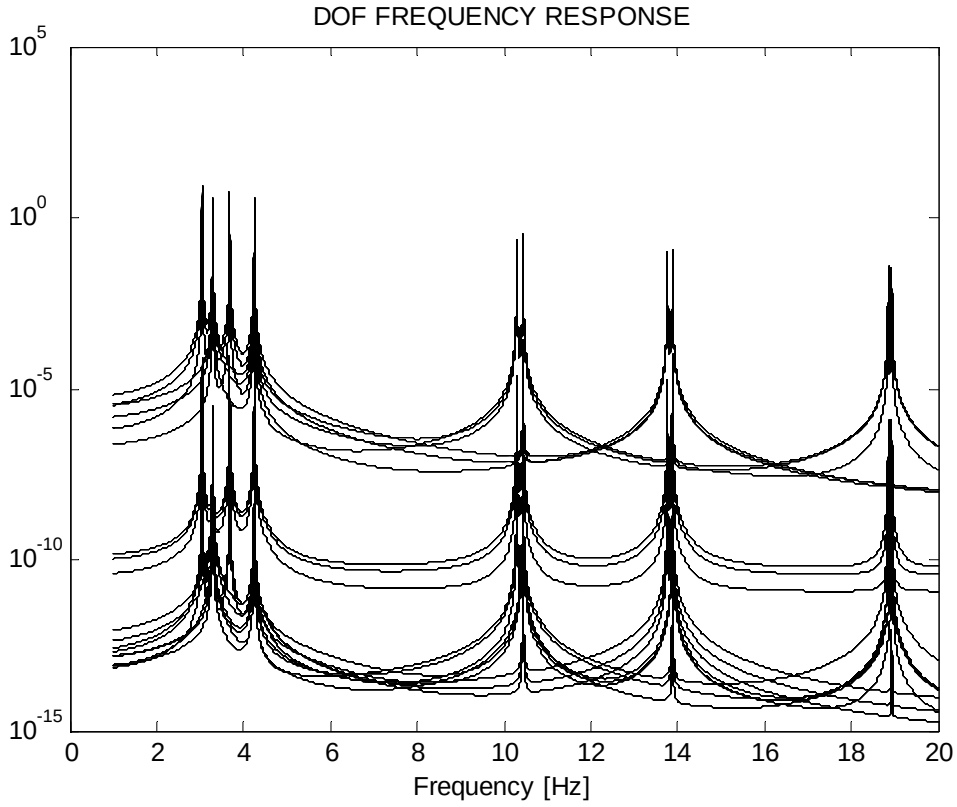

Figure 9: the response function of the structural degrees of freedom evaluated for a damping of $\nu=10^{-4}$

From the frequency response functions of the model, the four indexes $i_h(f)$ were computed, while a target function $T(f)$ for the neural network was defined as

$$T(f)=\frac{10^{t(f)}-1}{9}, \quad t(f)=\sum_{h=1}^{N_r}\exp\left[-\left(f-f_{r,h}\right)^2/\sigma^2\right] \tag{7}$$

where N_r is the number of eigenfrequencies $f_{r,h}$ considered (in the case at hand, the first 10 eigenfrequencies were considered); f is the frequency and σ a proper decay parameter.

The choice of the decay parameter σ was made on the basis of some considerations on the shape of the structural FRFs; since this parameter affects the width of the peaks that indicate the resonance frequencies, σ was determined to keep as separated as possible the pairs of close resonances around 10, 14 and 19 Hz in the target function (Figure 10). Correspondingly, the target function should exhibit pairs of close peaks, which can only be possible for $\sigma^2 \leq 0.001$.

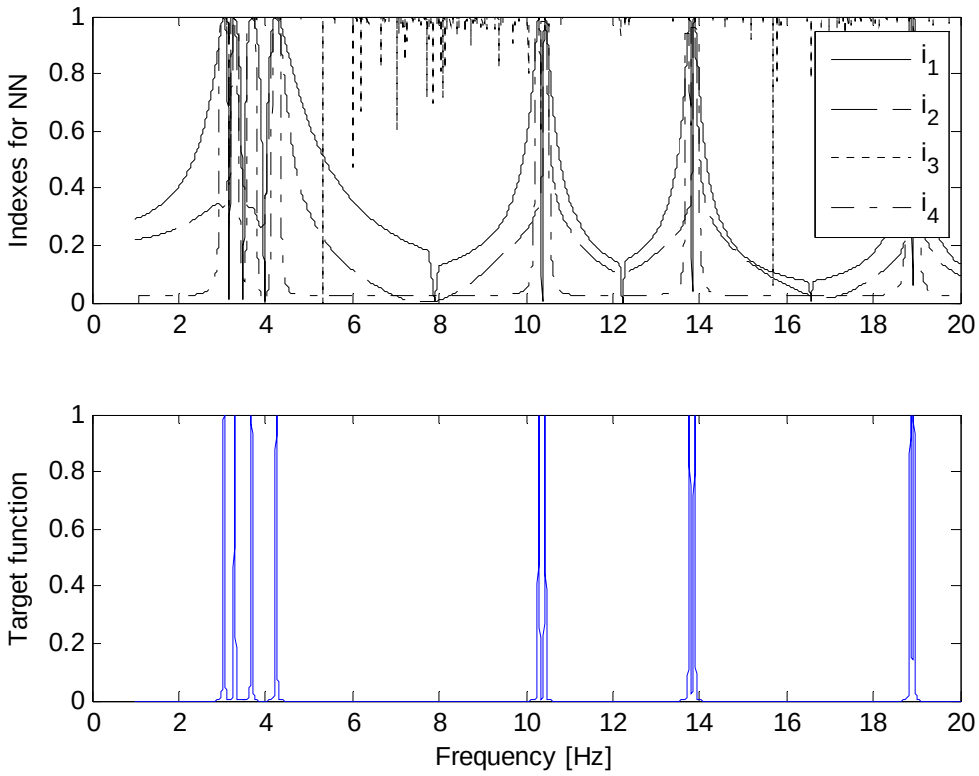

Figure 10: the four indexes obtained for the FEM model and the target function

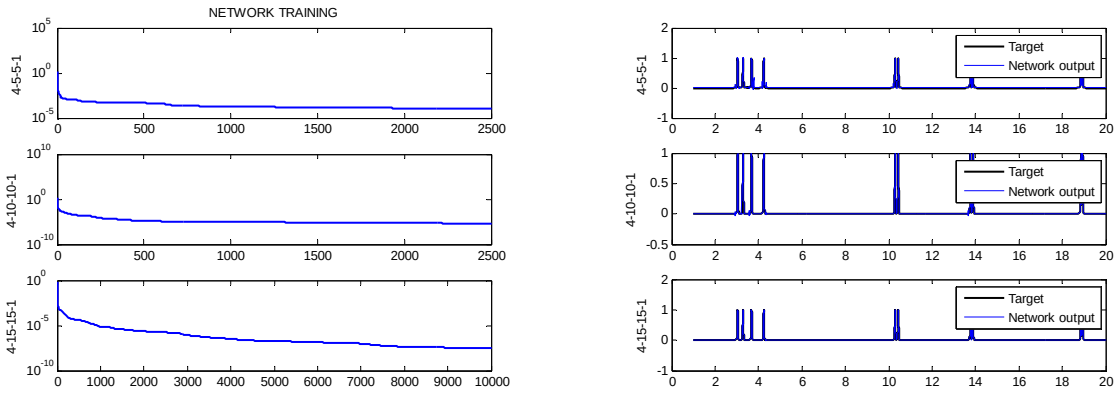

Figure 11: on the left, the performance of different networks during the training phase; on the right, the network output after the training phase (blue line) compared to the target function (thick black line)

Training was based on the Levemberg-Marquardt algorithm and employed as long as 10000 epochs in the most difficult cases.

Network validation was carried out on another structure (the shear type frame shown in Figure 12) and showed that two kinds of errors can arise: the presence of a natural frequency where there is no actual eigenfrequency, and the absence of a natural frequency where it should be present.

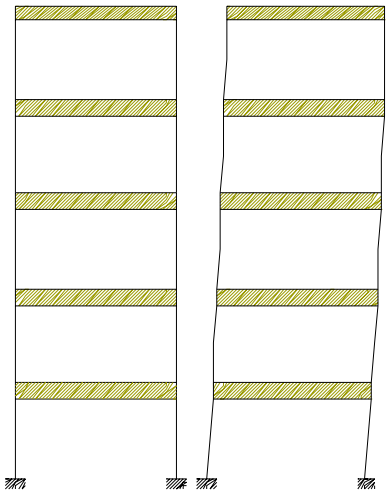

Figure 12: The validation structure with its first modal shape.

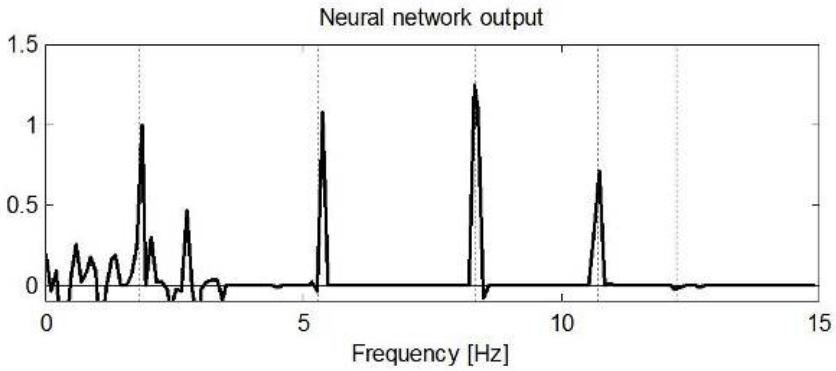

Figure 13: Example of validation of the 4-15-15-1 NN.
Structural resonances are denoted by dashed vertical lines.

Figure 13 shows an example of both types of error: at a frequency of about 3 Hz a false eigenfrequency is detected, and the last eigenfrequency is not detected at about 12 Hz. It must be noted that network validation was performed on 3 different data sets, and the other two gave good results.

The validation results show that the network output must be considered (when properly normalized) as an estimation of the probability of finding a structural resonance at a given frequency, rather than the certain presence or absence of eigenfrequencies.

In this light, it is useful to perform more than one test on the investigated structure: the analysis of the time histories of each test will give as many likelihood functions for the presence of structural resonances.

4 OUTPUT-ONLY IDENTIFICATION PROCEDURE

4.1 Signal analysis

The analysis of accelerometer signals is the first of two steps that constitute the identification procedure.

The recorded signals were transferred into a portable computer via a cross-cable. Then, the signals were digitally low-pass filtered at 12.5 Hz and resampled at 25 Hz. Spectral densities were evaluated by means of nonparametric estimation using different windows (Hanning, Hamming, DPSS and Blackman) and successively applying Fast Fourier Transform (FFT) to windowed data; with the exception of the periodogram (which is more sensitive to bias), no significant difference could be noticed in the evaluated spectral densities (Percival and Walden 1993 [8]), see Figure 14.

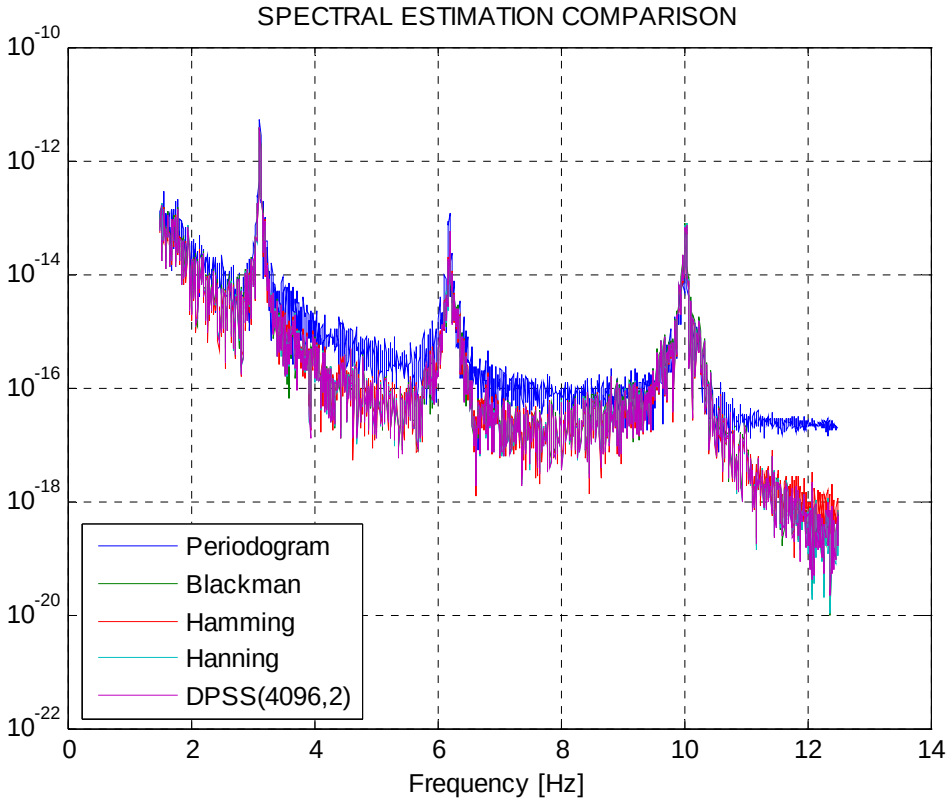

Figure 14. Comparison of the estimates of the spectral density of signal #2 with different data tapers.

The results obtained in the following analyses were also similar, so the data taper given by discrete prolate spheroidal sequences (4096,2) (Percival and Walden 1993 [8]) was adopted. The spectral densities were divided by a factor of $(2\pi)^4$ in order to evaluate the displacement spectra and the indicators previously descripted, $i_1(f)$ to $i_4(f)$, were estimated.

Figure 15 shows that the fourth index is capable of detecting resonances (one of the first identification methods, the peak picking, was based on this criterion), but shows also a certain width of its peaks, thus affecting the reliability of the estimate. The first index is close to 1 very often, but in proximity of structural resonances decreases rapidly when the frequency differs from the eigenfrequency; further useful indications come from the second and third indexes.

4.2 Combination of network output for different tests with same level of damage.

Since the neural network can undergo different kinds of errors, as pointed out before, for each level of damage several recordings of environmentally induced accelerations were taken.

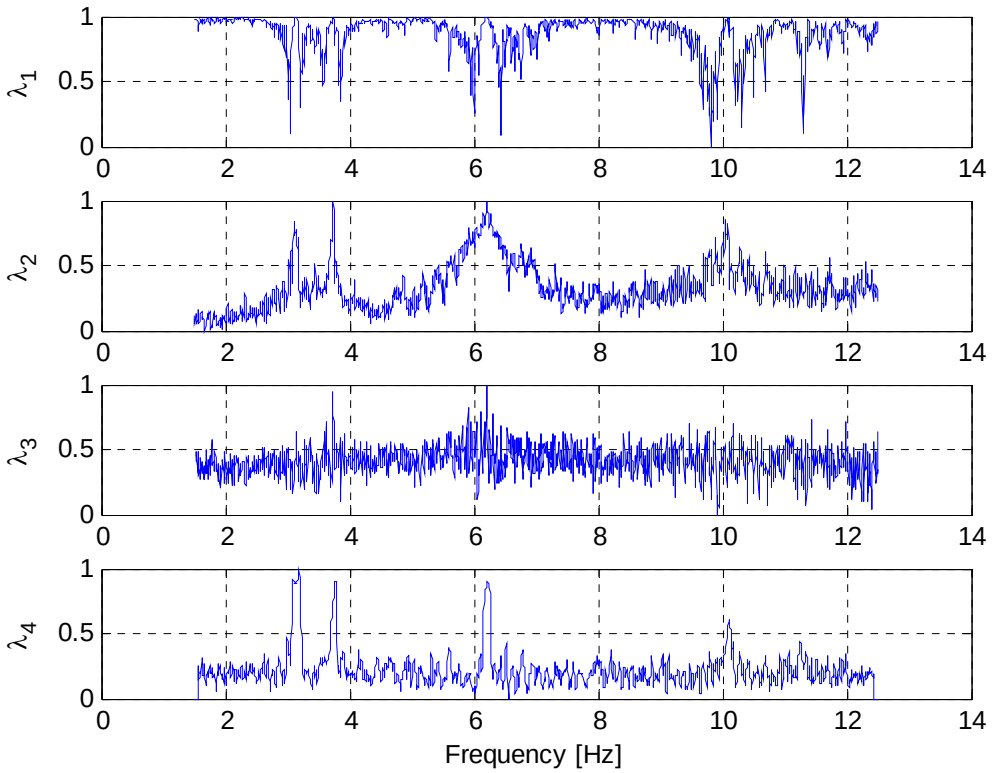

Figure 15: The four indexes as evaluated from the analysis of the signals recorded during the third test.

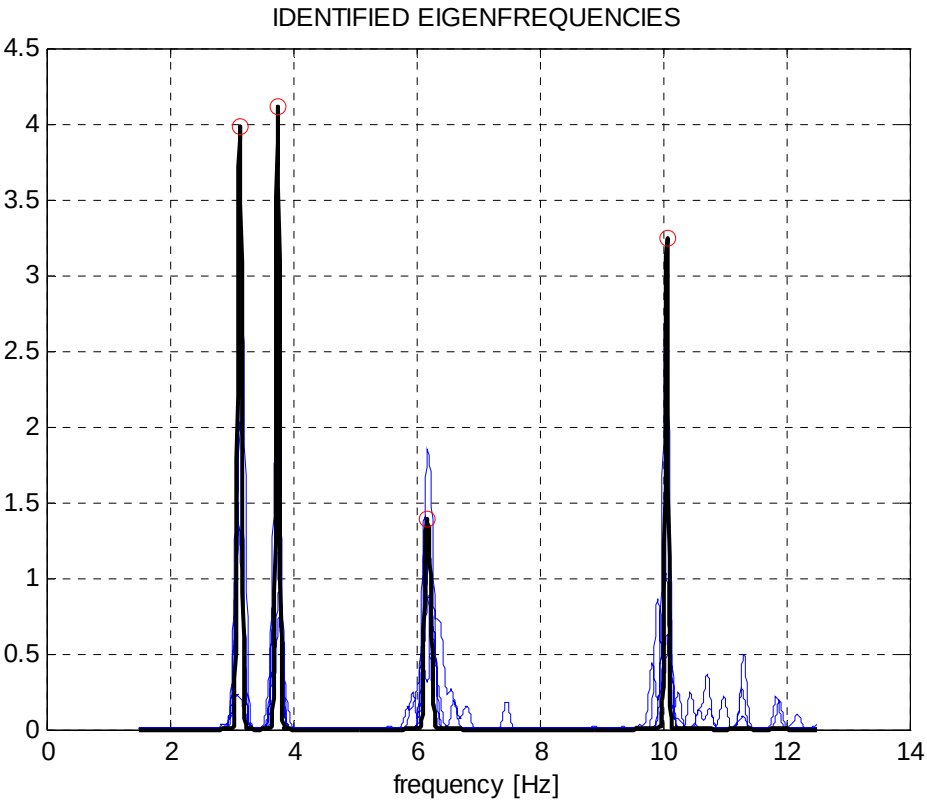

Figure 16: *Pdf* of structural resonance: first set of tests (undamaged structure)

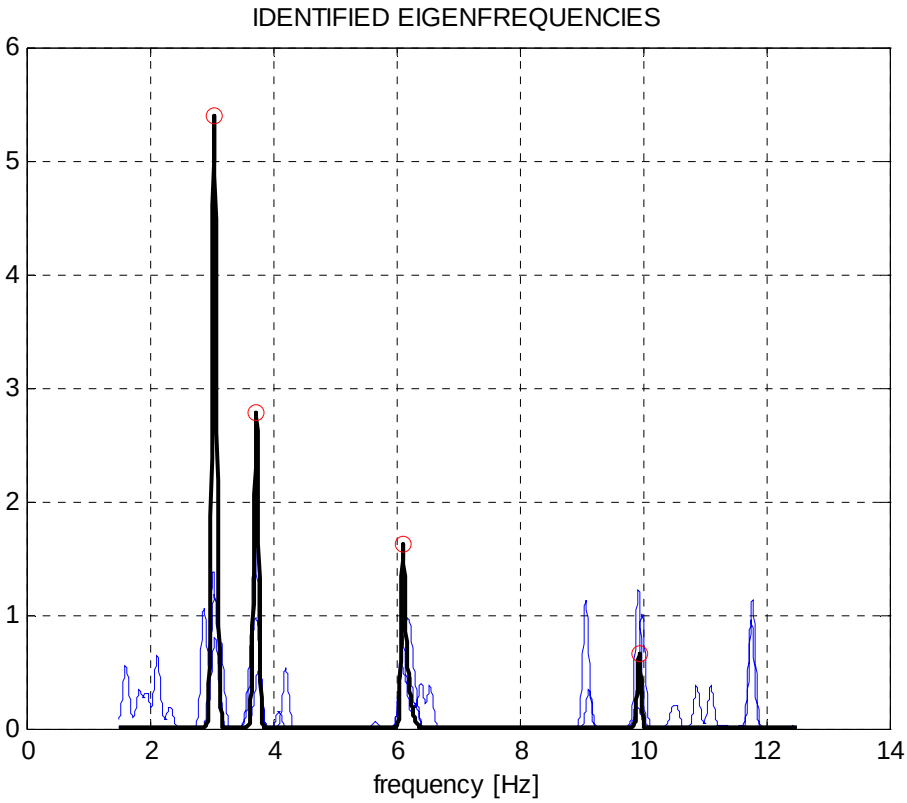

Figure 17: *Pdf* of structural resonance: third set of tests (third level of damage)

The results given by the network for each recording were therefore combined from a Bayesian point of view. Before the first recording was taken (for each level of damage), no assumptions about the distribution of structural eigenfrequencies were made, and therefore a uniform probability density for the eigenfrequency positions was considered.

The output of the neural network after each test brings information about the location of structural eigenfrequencies, but can be affected by errors. Therefore, it can be considered as an estimate of the likelihood to find a structural eigenfrequency at each frequency of interest.

The result is the final probability density function for the presence of eigenfrequencies. Figure 16 and Figure 17 show the likelihood functions coming out of each test of a given set (blue lines) and the final pdf for the structural resonances (thick black line).

It is worth spending some words on the results shown in Figure 18, where the evolution of the probability density of the first two structural eigenfrequencies is plotted.

Set #	f^{I} (Hz)	f_2 (Hz)	f_3 (Hz)	f_4 (Hz)
Set #0	3.14	3.76	6.18	10.06
Set #1	3.08	3.75	6.24	9.98
Set #2	3.09	3.71	6.20	9.96
Set #3	3.05	3.74	6.11	9.94
Set #4	3.03	3.72	6.13	9.91

Table 3. Main identified frequencies.

The probability density in the undamaged state is represented by the blue line, and shows peaks located at the highest values of the two resonances; they are also more narrow than the other ones, implying a higher reliability of the estimate.

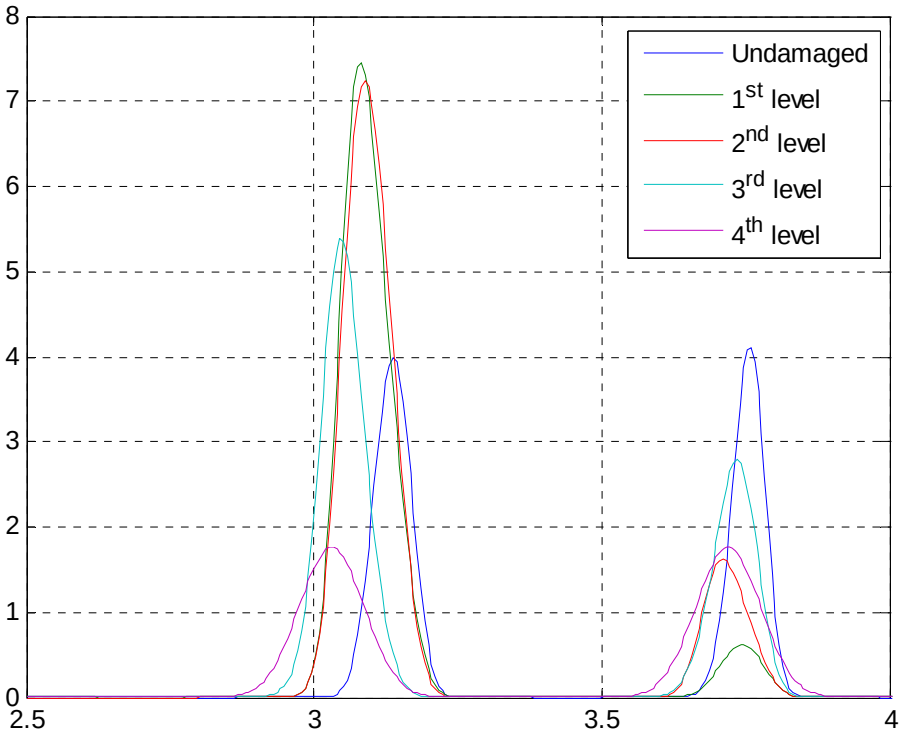

Figure 18: Evolution of probability density of the first two resonances with increasing damage

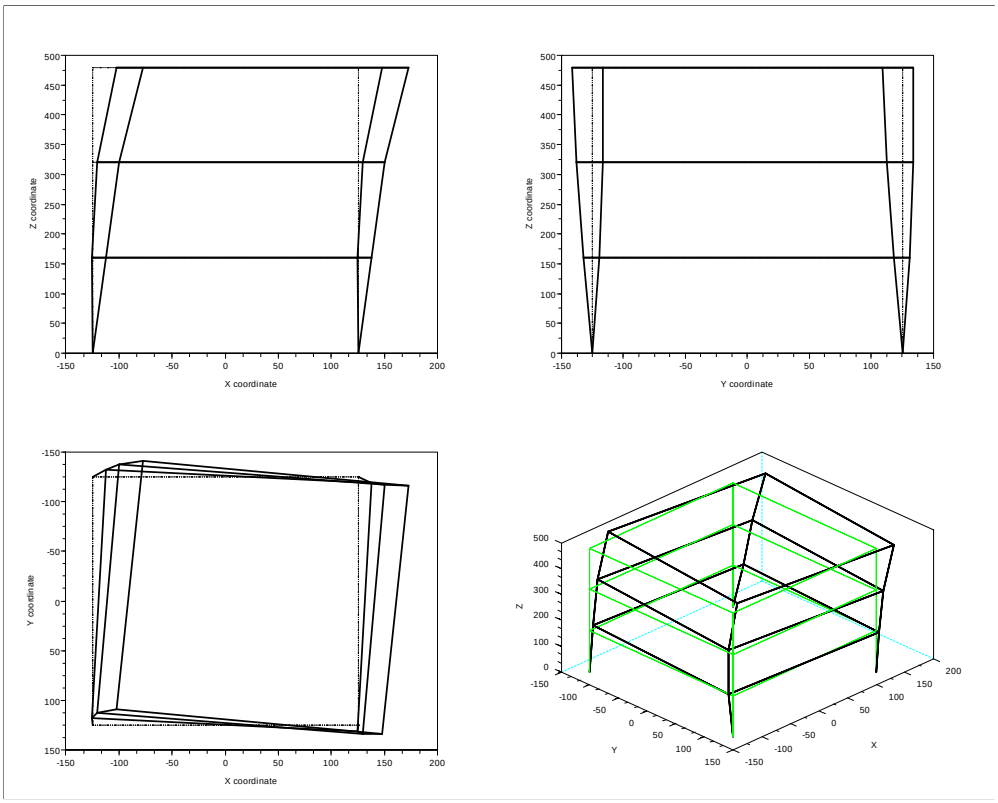

Figure 19: First bending mode (x-direction) - f_1=3.14 Hz

As it is clear also from Table 3, it is interesting to note that the second eigenfrequency estimate does not always decrease with increasing damage: as a matter of fact, it shows a minimum for set # 2 (2nd level of damage). But if we look at Figure 18, it can be noticed that the peaks relative to set #1 and set #2 estimate of the second eigenfrequency are a bit wider than the others, meaning a less reliable estimate.

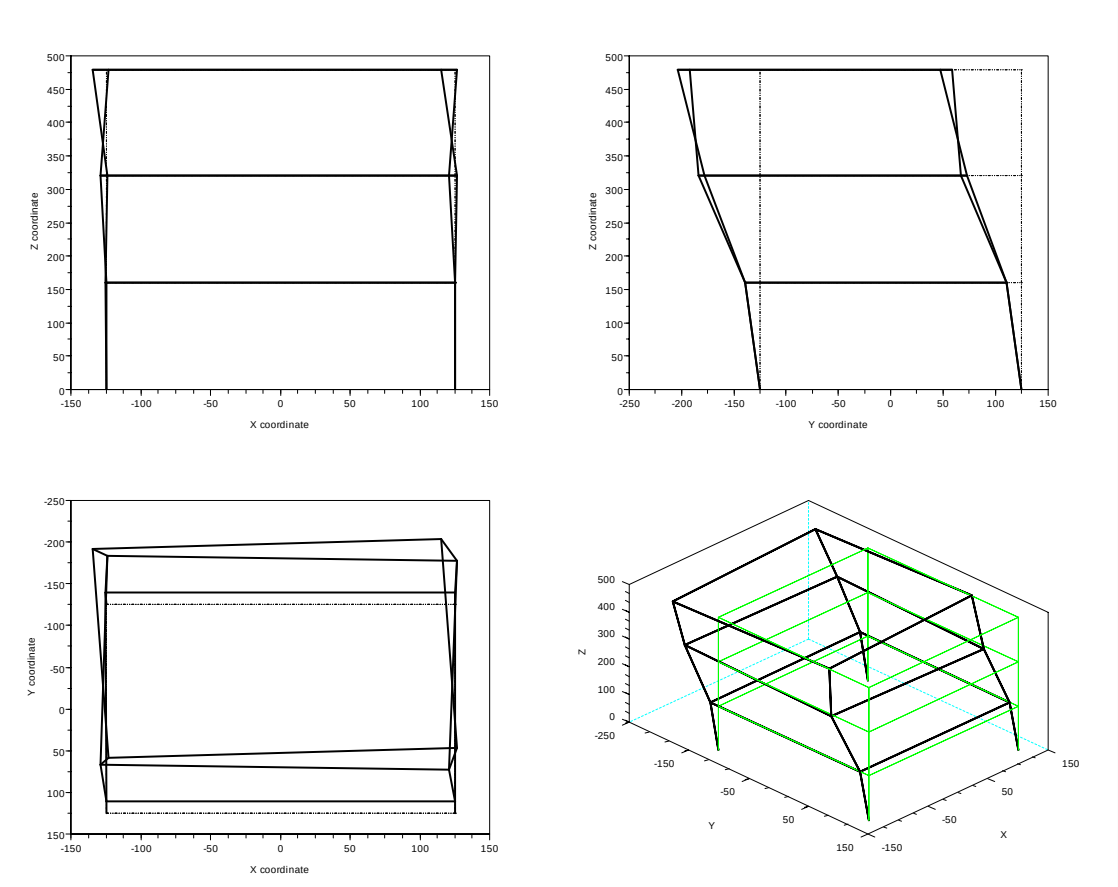

Figure 20: First bending mode (y-direction) - f_2=3.76 Hz

The same considerations hold also for the variation of the torsional frequency, f_3. The exact relation between the width of the peaks and the estimate reliability is currently under examination. Once the eigenfrequencies were estimated, the corresponding modal shapes could be retrieved by means of the spectral SVD. The first three estimated modal shapes for the undamaged state of the frame are reported in Figure 19, Figure 20 and Figure 21.

The obtained results have been compared with those given by SSI in the output-only, covariance-driven form. Even in the case of SSI the stabilization diagram can be used to define the probability density of structural resonance. The *pdf* could be built by means of a Gaussian base according to Eq. (8) where O_{min} and O_{max} represent the minimum and maximum order of the SSI model and N_f is the number of identified main frequencies.

Figure 22 is an example of the stabilization diagram and the *pdf* of structural resonance as calculated for the specimen it its initial configuration (i.e. without damage).

$$p(f) = K \sum_{h=O_{\min}}^{O_{\max}} \sum_{k=1}^{N_f} \exp\left(-\frac{(f - f_{hk})^2}{2\sigma_h^2} \right)$$

$$K = \left[\int_{-\infty}^{\infty} \sum_{h=O_{\min}}^{O_{\max}} \sum_{k=1}^{N_f} \exp\left(-\frac{(f - f_{hk})^2}{2\sigma_h^2} \right) df \right]^{-1} \tag{8}$$

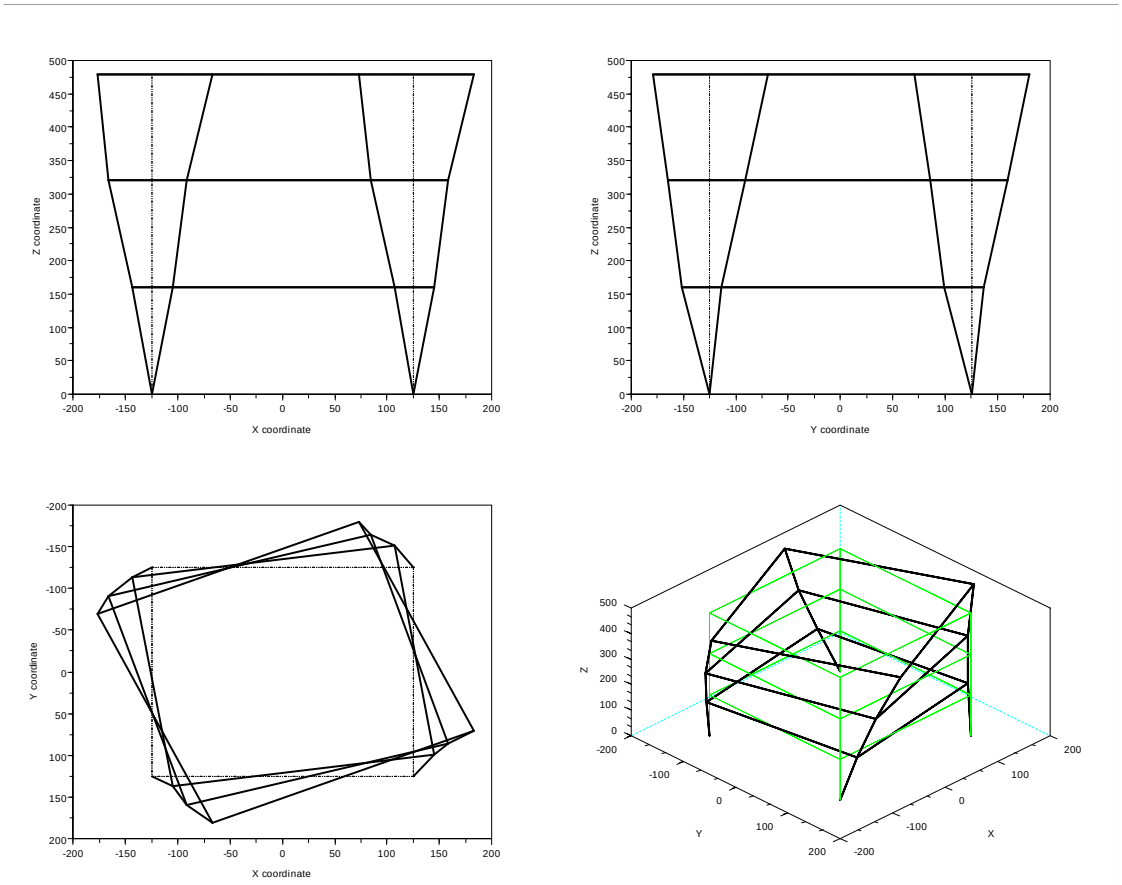

Figure 21: First torsional mode (x-y plane) - f_3= 6.18 Hz

Table 4 reports the first three identified frequencies for representative tests of each damage level. The increasing level of damage (being the column's flange cut) interests mainly the frequency in the x-direction (Figure 18) and the torsional one.

Test #	f_1 (Hz)	f_2 (Hz)	f_3 (Hz)
Test # 1	3.12	3.75	6.28
Test #32	3.08	3.72	6.16
Test #41	3.04	3.72	6.14

Table 4: Main identified frequencies (SSI).

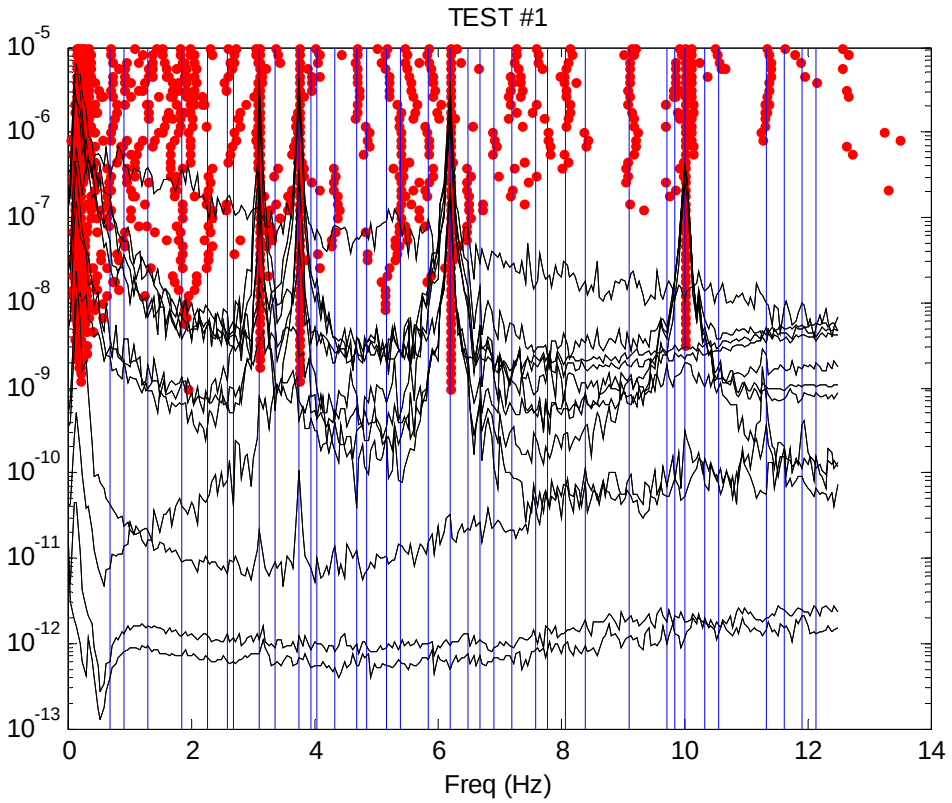

Figure 22: Stabilization diagram together with autospectra of the recorded acceleration signals: test #1

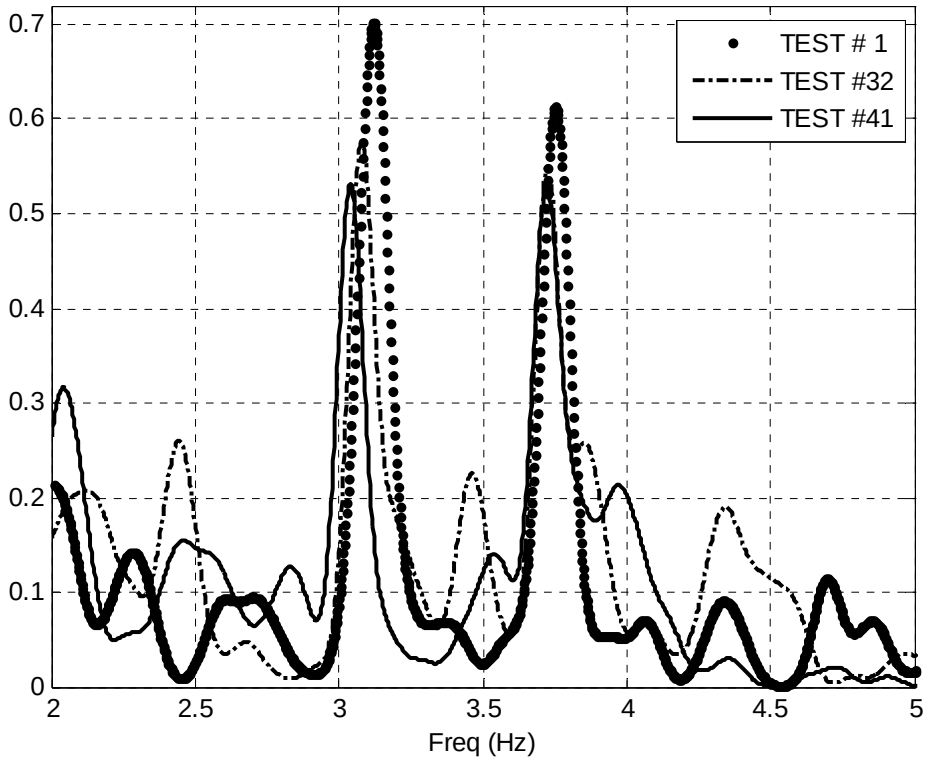

Figure 23: *Pdf* of the first two structural resonances: test #1, 32, 41

Figure 23 reports the *pdf* of the two first structural resonances in case of damage (test #32 &41) compared with the case without damage (test #1).

5 NEXT RESEARCH STEP: GENETIC ALGORITHM

Next steps of the research aim to propose the employment of genetic algorithms (GA) techniques for the identification of a finite element model of the specimen, as GA has been shown to be able to overcome the limitations of traditional methods (see e.g. Faravelli *et al*.[7]).

Genetic algorithms are based on ideas from the science of genetics and the process of natural selection. They work with an initial population (strings of zeros and ones i.e. binary strings) which may correspond to certain numerical values of a particular variable whose size is depending on the problem under consideration. The initial population is generated randomly; each string in the population corresponds to a chromosome and each binary element of the string to a gene. A new population is developed starting from the initial population according to the processed that are analogue to the fundamental genetic processes: a) reproduction based on fitness, b) crossover and c) mutation.

A set of chromosomes is selected at the reproduction stage and members of the population are chosen for reproduction on the basis of their fitness: the fittest have a greater probability of reproducing in proportion to the value of their fitness. The process of reproduction is implemented by using the crossover. Many crossover techniques are available using different data structures (single crossover point or many cross-over points). The mutation is a process where randomly a particular gene in a particular chromosome is changed. The process of mutation in a genetic algorithm occurs very rarely and hence this probability of a change in a string is normally kept very low. Nevertheless the purpose of mutation is to preserve and introducing diversity. From a computational point of view mutation should allow the algorithm to avoid local minima by preventing the population of chromosomes from becoming too similar to each other, thus slowing or even stopping evolution. Crossover and mutation represent the two special features that make different a genetic algorithm with respect to a traditional direct search procedure and make it interesting for optimization and search problems.

$$F = \sum_{i=1}^{k} \left[p_{\lambda,i} \cdot \left(\frac{\lambda_{F,i} - \lambda_{Exp,i}}{\lambda_{F,i}} \right)^2 + p_{\phi,i} \cdot \left(1 - MAC(i,i)\right)^2 \right]$$
$$MAC(i,i) = \frac{\left(\boldsymbol{\varphi}_{Fi}^{t} \cdot \boldsymbol{\varphi}_{Expi}\right)^2}{\left(\boldsymbol{\varphi}_{Fi}^{t} \cdot \boldsymbol{\varphi}_{Fi}\right) \cdot \left(\boldsymbol{\varphi}_{Expi}^{t} \cdot \boldsymbol{\varphi}_{Expi}\right)} \tag{9}$$

CONCLUSIVE REMARKS

The paper has discussed some recent advances in case of "output-only" systems aimed at the damage identification of structural systems. To this aim the experimental campaign conducted in a benchmark three-story steel structure at the Civil Engineering Laboratory of the University of Florence (Italy) laboratory is currently carried out and has been reported on. The benchmark structure has been tested (under ambient loading) starting from the actual configuration and imposing steps of increasingly damage level by partial cuts of flanges on some steel elements (columns). Successively a neural network based procedure has been proposed

and employed to analyse accelerometer signals recorded during the experimental campaign. Results are discussed and the dynamic properties of the building are evaluated at each damage level. At the end, the ongoing research step aimed to employ genetic algorithms to finite element model identification has been discussed.

ACKNOWLEDGMENTS

The authors wish to thank Mr. Saverio Giordano (Civil Engineering Laboratory of the Department of Civil and Environmental Engineering) for his precious assistance and cooperation during the whole experimental campaign.

REFERENCES

[1] A. Deraemaeker, E. Reynders, G. De Roeck, J. Kulla, Vibration-based structural health monitoring using output-only measurements under changing environment. *Mechanical Systems and Signal Processing*, **22**, 34-56, 2008.

[2] A. Alvandi, C. Cremona, Assessment of vibration-based damage identification techniques. *Journal of Sound and Vibration*, **292**, 179–202, 2006.

[3] L. Facchini, M. Betti, P. Biagini, Neural networks for output-only parameter identification. B.A. Schrefler & U. Perego eds. *8th World Congress on Computational Mechanics (WCCM8) & 5th European Congress on Computational Methods in Applied Sciences and Engineering (ECCOMAS 2008)*, Venice, Italy, June 30 – July 4, 2008.

[4] L. Facchini, M. Betti, P. Biagini, Studi recenti nell'identificazione 'output only' di strutture vibranti mediante l'impiego di reti neurali. A.L. Materazzi, M. Breccolotti, F. Cluni, F. Ubertini, I. Venanzi eds., *3° Workshop sui Problemi di vibrazioni nelle strutture civili e nelle costruzioni meccaniche*, Perugia, Italy, September 11-12, 2008.

[5] J.S. Bendat, A.G. Piersol, *Engineering Applications of Correlation and Spectral Analysis*. Wiley, Interscience, 1993.

[6] B. Peeters and G. De Roeck (1999), "Reference-based stochastic subspace identification for output-only modal analysis", Mechanical Systems and Signal Processing 13(6), 855-878, 1999.

[7] L. Faravelli, F. Materazzi, M. Rarina, Genetic algorithms for structural identification. *ICOSSAR 2005*, Roma, Italy, June 19-23, 2005.

[8] D. B. Percival, A. T Walden, *Spectral Analysis for Phisical Applications*. Cambridge University Press, Cambridge 1993.

[9] R. Brincker, L. Zhang, P. Andersen, Modal Identification from Ambient Responses using Frequency Domain Decomposition. *Proceedings of the 18th International Modal Analysis Conf.*, San Antonio, USA, 2000.